Supplemental Figures and Text

Regulation of Mouse Oocyte Microtubule and Organelle Dynamics by PADI6 and the Cytoplasmic Lattices

Rui Kan, Piraye Yurttas, Boram Kim, Bora Lee, Luccie Wo, Roger Gosden, and Scott A. Coonrod.

SUPPLEMENTAL FIGURES AND LEGENDS

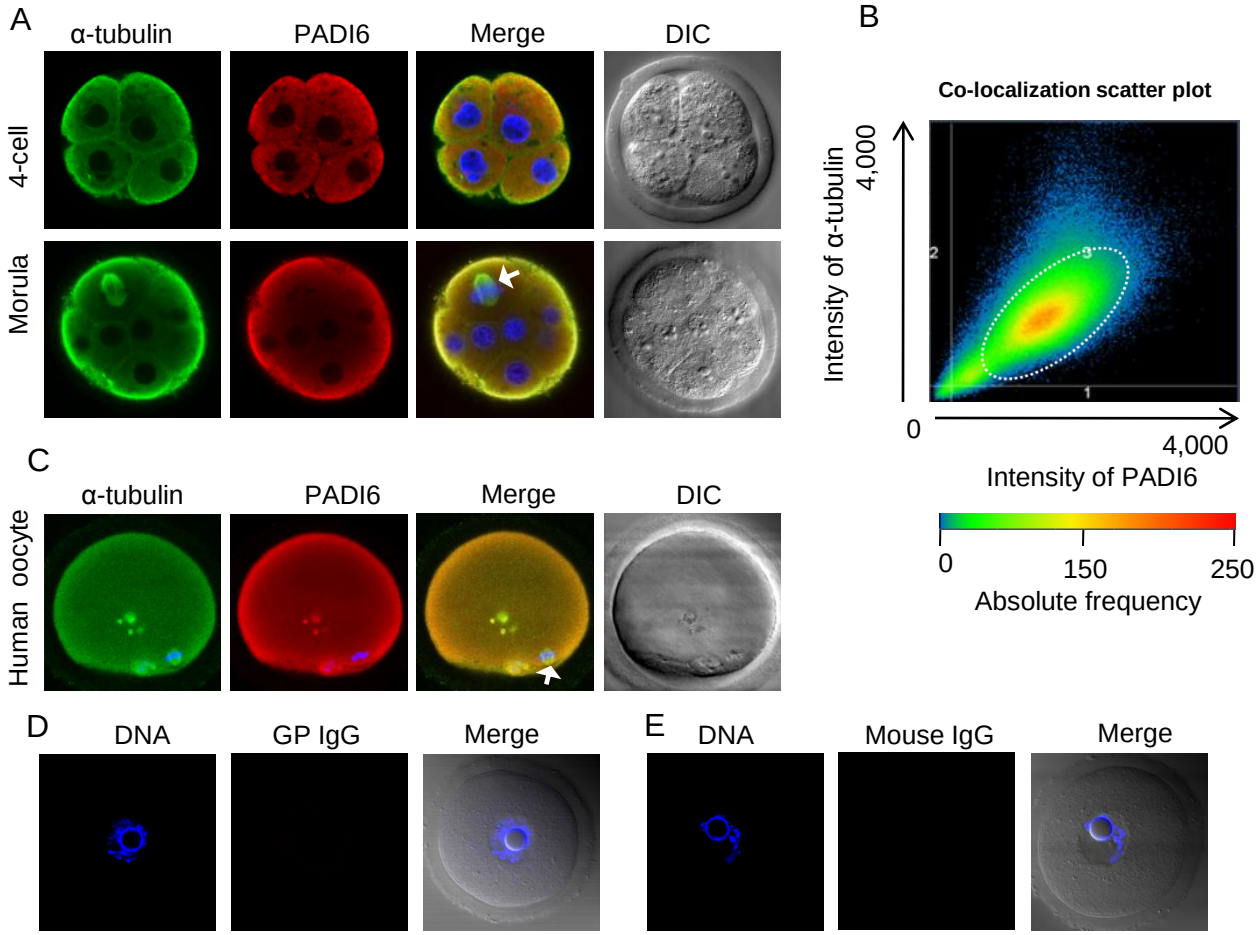

Figure S1. Co-localization of PADI6 and α-tubulin in murine early embryos and human mature oocytes. (A) Co-localization of α-tubulin and PADI6 by confocal microscopy in mouse embryos. The co-localization is highlighted in merged images. (B) The co-localization scatter plot of α-tubulin and PADI6 in mouse oocytes. The degree of co-localization is shown in oval. (C) Co-localization of α-tubulin and PADI6 in human ovulated mature oocytes by confocal microscopy. The co-localization pattern is shown in yellow in merge panel. Arrow indicates spindle MTs. (D) Confocal indirect immunoflourescence staining was not observed when oocytes were incubated with similar concentrations of either (D) guinea pig Ig G (control for anti-PADI6 antibody) or (E) mouse Ig G (control for anti-α-tubulin antibody).

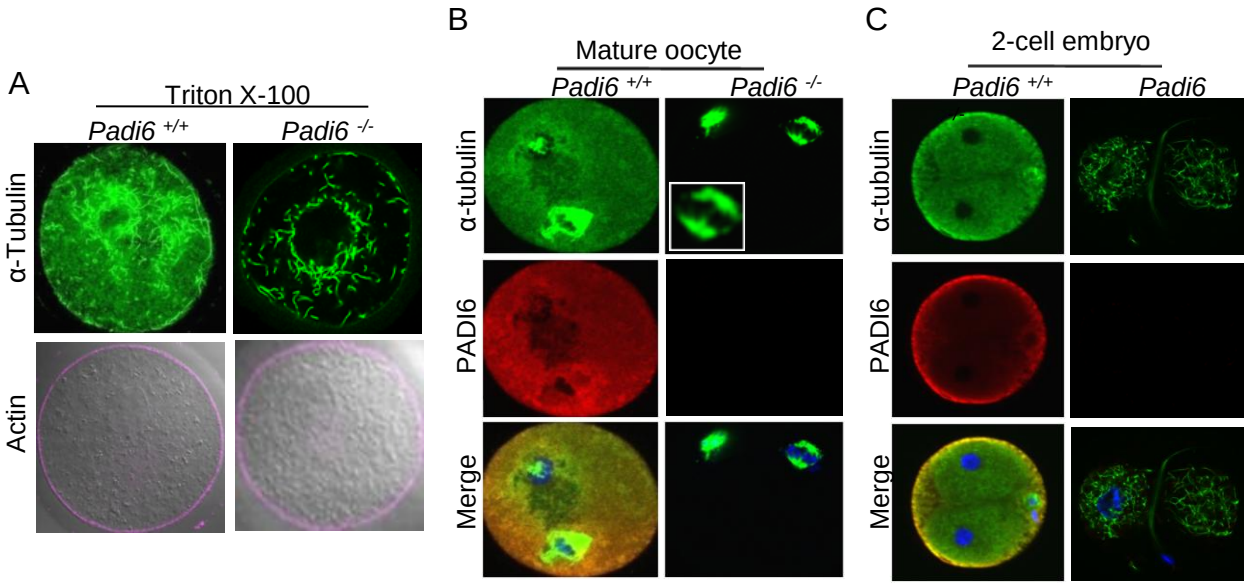

Figure S2. Triton X-100 solubility of tubulin is increased in *Padi6*-deficient mature oocytes and two-cell embryos. (A) Confocal images of actin and α-tubulin in wild-type and *Padi6*-null GV oocytes. Actin was stained with phalloidin Alexa Fluor 633 suggested the microfilaments were not strongly affected in *Padi6*-null oocytes. (B) IIF-confocal analysis of staining levels of a-tubulin and PADI6 following Triton X-100 extraction in wild-type and *Padi6*-null mature oocytes. (C) Same as (B) except using two-cell embryos. Experiments were repeated at least three times.

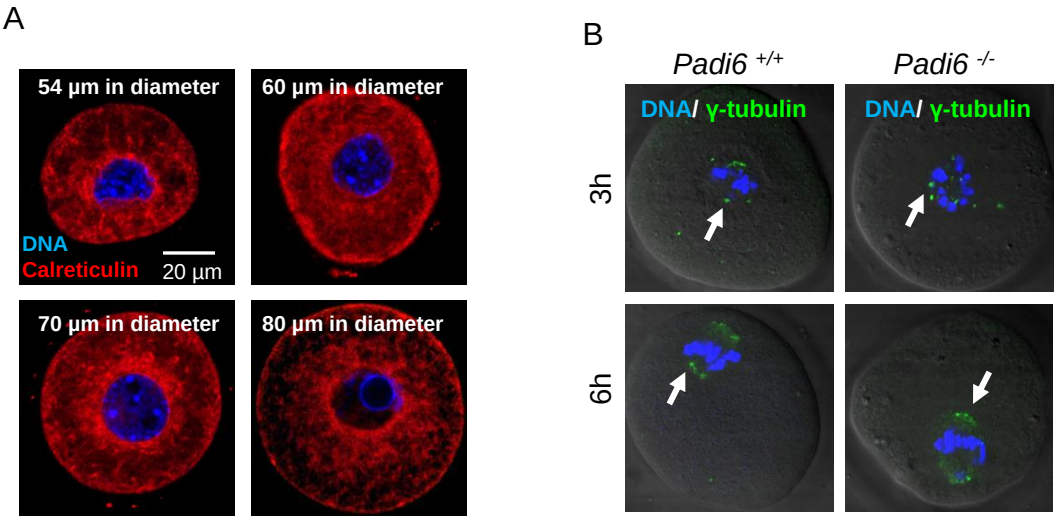

Figure S3. ER localization in growing wild type oocytes and gamma-tubulin localization during maturation of wild type and PADI6-null oocytes. (A) Confocal immunoflourescence localization of calreticulin in incompetent growing and competent, fully grown wild-type oocytes. Growing oocytes (<80 µm in diameter) were isolated from the ovaries of 2 week old wild type females and fully grown oocytes were isolated from the ovaries of PMSG-primed 4-7 week old females. (B) Confocal immunoflourescence localization of gamma-tubulin in wild-type and *Padi6*-null oocytes after 3 and 6 hours of in vitro maturation. Arrows indicate the tubulin foci.

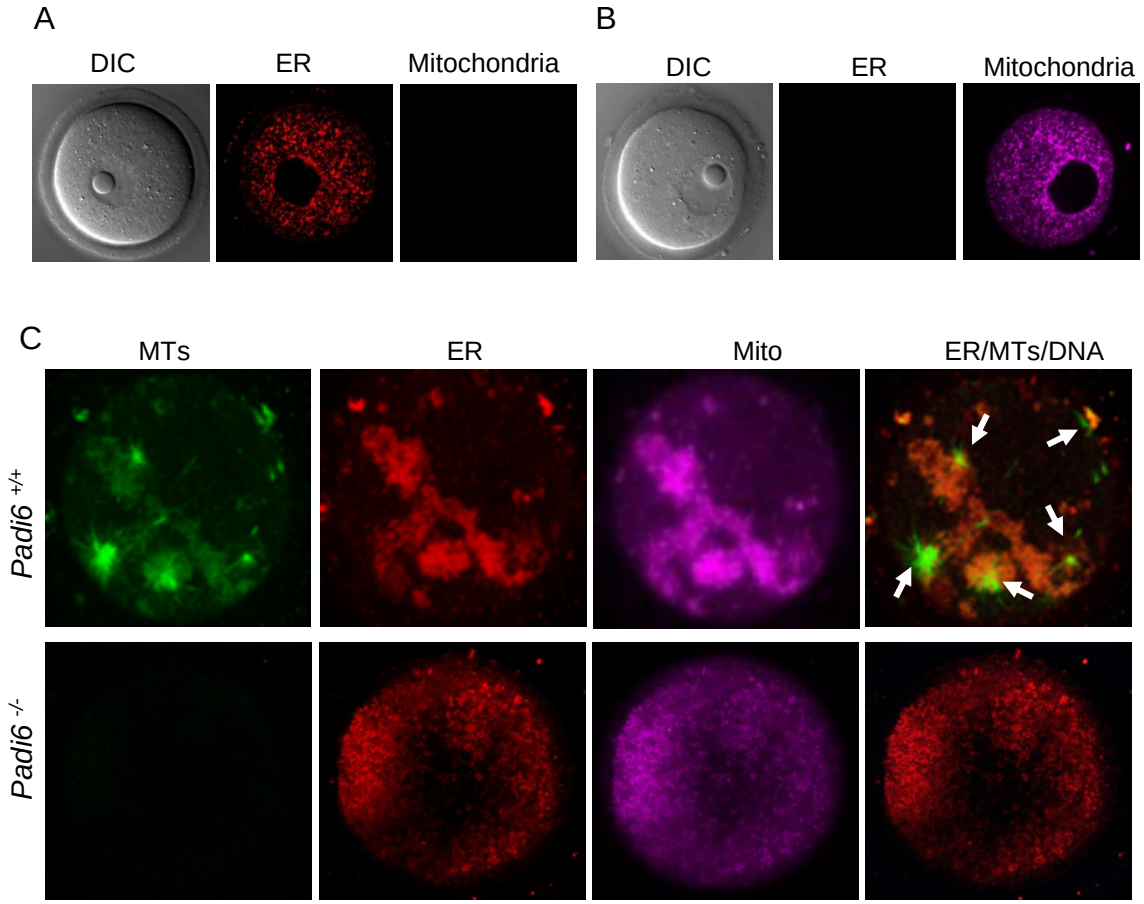

Figure S4. Validation of confocal parameters for live staining of oocyte organelles and redistribution of ER and mitochondria in taxol-treated mouse mature oocyte. (A) Confocal filter settings were configured for Mito-tracker and oocytes were then stained with Mito-tracker alone. (B) Confocal filter settings were configured for ER tracker and oocytes were then stained with ER tracker alone. No bleed-through was observed between the red and far-red channels. Experiments were repeated two times. (C) Localization of ER and mitochondria in the cytoplasm of taxol-treated mouse mature oocytes by confocal microscopy. Arrows indicate the re-localization of the organell around cytoplasmic asters.

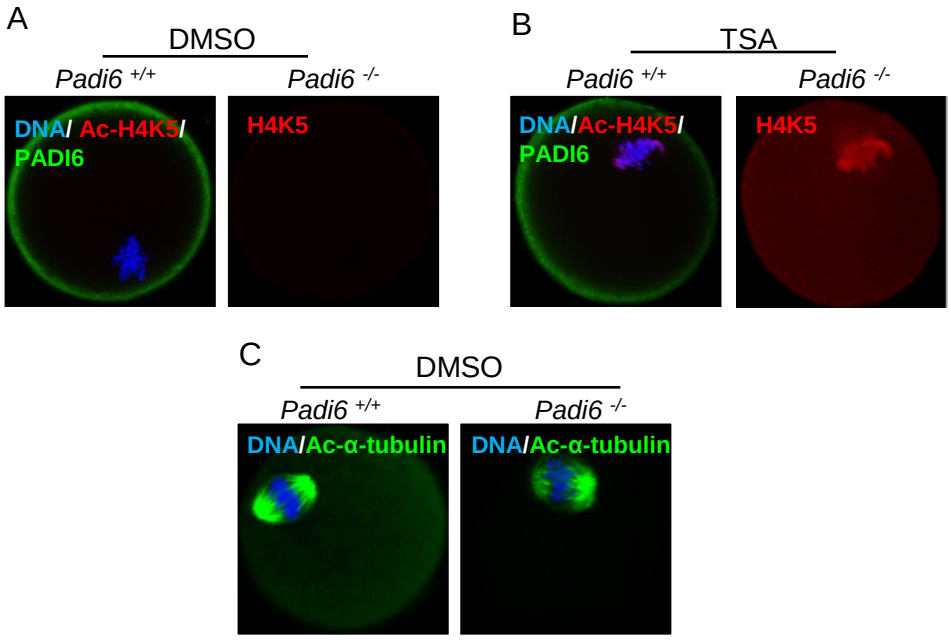

Figure S5. Acetylated H4K5 staining in TSA-treated mouse oocytes and acetytelated-tubulin staining in DMSO-treated oocytes. (A-B) Acetylated H4K5 staining in wild-type and mutant PADI6 oocytes after DMSO and TSA treatment. Acetylated H4K5 was shown in red and PADI6 was shown in green. (C) Acetylated tubulin staining in wild-type and mutant PADI6 oocytes after DMSO treatment. Experiments were repeated two times.

Movie S1. Time-lapse fluorescence movie of mitochondrial dynamics in GV stage wild type and PADI6-null oocytes. GV stage wild type (WT) and PADI6-null (KO) oocytes were stained with Mito-Tracker for 30 min in MEM-alpha medium plus 5% FBS and imaged at the interval of a millisecond for 5 min using Zeiss confocal microscopy.

Movie S2. Time-lapse movie of lipid droplet dynamics during maturation of wild type and PADI6-null oocytes. GV stage wild type (WT) and PADI6-null (KO) oocytes were matured in MEM-alpha medium plus 5% FBS and imaged at the interval of a minute for 12 hours using Zeiss light microscopy.

Table S1. Co-localization of α-tubulin and PADI6 following Triton X-100 extraction.

Scatter Region	Number Pixels	Mean Intensity PADI6(±S.D.)	Mean Intensity tubulin(±S.D.)	Colocalization Coefficient PADI6	Colocalization Coefficient tubulin	Manders' Overlap Coefficient	Pearson's Correlation R
1	3174	417±105	207±38				
2	1830	236±41	348±90				
3	443567	1490±467	1274±471	0.993	0.996	0.97	0.7

Scatter region 1: pixels in PADI6 channel only.
Scatter region 2: pixels in α-tubulin channel only.
Scatter region 3: co-localizing pixels.